Article:

Lyons, T.P., Gillard, D.J. orcid.org/0000-0002-0001-4918, Leblanc, C. et al. (11 more authors) (2022) Giant effective Zeeman splitting in a monolayer semiconductor realized by spin-selective strong light–matter coupling. Nature Photonics, 16 (9). pp. 632-636. ISSN 1749-4885

https://doi.org/10.1038/s41566-022-01025-8

This is a post-peer-review, pre-copyedit version of an article published in Nature Photonics. The final authenticated version is available online at: http://dx.doi.org/10.1038/s41566-022-01025-8.

Giant effective Zeeman splitting in a monolayer semiconductor realized by spin-selective strong light-matter coupling

T. P. Lyons,[1, 2, 3, *] D. J. Gillard,[1, 3] C. Leblanc,[4, 3] J. Puebla,[5] D. D. Solnyshkov,[4, 6] L. Klompmaker,[7] I. A. Akimov,[7, 8] C. Louca,[1] P. Muduli,[9, 10] A. Genco,[1] M. Bayer,[7, 8] Y. Otani,[5, 11] G. Malpuech,[4] and A. I. Tartakovskii[1, †]

[1] *Department of Physics and Astronomy, The University of Sheffield, Sheffield S3 7RH, UK*
[2] *Present address: RIKEN Center for Emergent Matter Science, Wako, Saitama 351-0198, Japan*
[3] *These authors contributed equally to this work*
[4] *Institut Pascal, PHOTON-N2, CNRS, Université Clermont Auvergne, F63000 Clermont-Ferrand, France*
[5] *RIKEN Center for Emergent Matter Science, Wako, Saitama 351-0198, Japan*
[6] *Institut Universitaire de France (IUF), F-75231 Paris, France*
[7] *Experimentelle Physik 2, Technische Universität Dortmund, 44221 Dortmund, Germany*
[8] *Ioffe Institute, Russian Academy of Sciences, 194021 St. Petersburg, Russia*
[9] *Institute for Solid State Physics, University of Tokyo, Kashiwa 277-8581, Japan*
[10] *Present address: Department of Physics, Indian Institute of Technology Madras, Chennai 600036, India*
[11] *Institute for Solid State Physics, University of Tokyo, Kashiwa, Chiba 277-8581, Japan*

(Dated: May 10, 2022)

Strong coupling between light and the fundamental excitations of a two-dimensional electron gas (2DEG) are of foundational importance both to pure physics and to the understanding and development of future photonic nanotechnologies [1–7]. Here we study the relationship between spin polarization of a 2DEG in a monolayer semiconductor, $MoSe_2$, and light-matter interactions modified by a zero-dimensional optical microcavity. We find pronounced spin-susceptibility of the 2DEG to simultaneously enhance and suppress trion-polariton formation in opposite photon helicities. This leads to observation of a giant effective valley Zeeman splitting for trion-polaritons (g-factor > 20), exceeding the purely trionic splitting by over five times. Going further, we observe clear effective optical non-linearity arising from the highly non-linear behavior of the valley-specific strong light-matter coupling regime, and allowing all-optical tuning of the polaritonic Zeeman splitting from 4 to > 10 meV. Our experiments lay the groundwork for engineering topological phases with true unidirectionality in monolayer semiconductors, accompanied by giant effective photonic non-linearities rooted in many-body exciton-electron correlations.

MAIN

Monolayer $MoSe_2$ presents a four-band massive Dirac system for studying spin and valley pseudospin dependent interactions between electrons, excitons, and photons [3, 4]. In the presence of an appreciable free carrier density, simple neutral exciton absorption evolves into two Fermi-polaron branches, repulsive and attractive [2–4, 7]. The monolayer then plays host to a Bose-Fermi mixture consisting of excitons dressed by electrons (or holes, for *p*-type doping). Strong coupling of these Fermi-polaron resonances to photonic microcavity modes has been demonstrated [4, 5]. Simplistically, the repulsive and attractive polarons correspond to a spin-triplet or spin-singlet interaction, respectively, between the two-dimensional electron gas (2DEG) and the constituent electron of the exciton [3, 4, 7]. In $MoSe_2$, subject to strict spin-valley locking and chiral optical selection rules, this has the consequence of tying the 2DEG degree of spin polarization to the oscillator strengths of the polaron resonances in opposite photon helicities. The extreme example of this effect is when the 2DEG becomes fully spin polarized, leading to vanishing absorption of the attractive polaron in one photon helicity [3, 7].

It has recently been reported that when the Fermi level is significantly smaller than the trion binding energy, the attractive polaron may be adequately described as a three-body charged exciton, or trion [8, 9]. Although nominally the trion exists only in the strict single particle limit, in reality the transition between these two quasiparticle regimes is unclear, and likely depends heavily on the degree of exciton and carrier spatial localization over the monolayer, especially at low densities. This is particularly true in the case of nonequilibrium scenarios such as photoluminescence experiments, in which both species may coexist [9].

Valley Zeeman splitting of these excitonic complexes has been reported under application of strong out-of-plane magnetic fields (B-fields) [3, 6, 10]. However, translating the relatively large Zeeman splitting of a purely matter-bound excitation into a photonic mode splitting remains a fundamental challenge not only in opto-valleytronics [11], but also in topological photonics. Indeed, many topological states of light have been implemented in recent years [12], including using TMD exciton-polaritons [13, 14]. The ultimate goal of real topological protection against any type of disorder scattering and back-reflection requires time-reversal symmetry breaking [15, 16], with the size of the topological gap limited by the effective Zeeman splitting of the photonic modes. Large splittings are difficult to achieve at optical frequencies, and in the existing realizations either based on the use of magnetic proximity effects [17] or on the matter-based Zeeman splitting of exciton-polaritons [18, 19], the topological gap was < 1 meV, too small to be clearly observable.

In our work, by harnessing many-body interactions in a 2-dimensional Bose-Fermi mixture, we realize a giant effective trion-polariton Zeeman splitting, over 5 times larger than the bare (uncoupled) trion splitting, and more than double the polariton linewidths, a crucial step towards elimination of unwanted coupling between chiral modes [20]. We moreover demonstrate giant effective non-linearity $\alpha \approx 0.2\pm0.05$ meV·µm^2 for trion-polaritons under a magnetic field. This value is one order of magnitude larger than previously reported in TMDs [5, 21] and is based on an original mechanism involving free carrier valley relaxation and strong light-matter coupling. Large photonic non-linearities, as in this work, are crucial for classical, quantum and topological photonics [12, 16].

We study a MoSe$_2$ monolayer on a 10 nm thick film of the ferromagnetic semiconductor europium sulfide (EuS) which coats a dielectric distributed Bragg reflector (DBR). Firstly, we characterize the MoSe$_2$ monolayer in the half-cavity, or bare flake, configuration, at temperature $T = 4.2$ K. Fig. 1a shows circular polarization resolved reflectance contrast (RC $= (R_0 - R)/R_0$, where R and R_0 are the reflectance from the MoSe$_2$ and adjacent EuS substrate, respectively) spectra from the sample under linearly polarized broadband illumination at out-of-plane magnetic field strengths $B = -8, 0, +8$ T. We observe, at $B = 0$ T, two clear absorption peaks attributed to the neutral exciton (X_{RC}) and trion (T_{RC}) at higher and lower energy, respectively. T_{RC} displays a significant spectral weight, indicating an elevated doping level of the flake. These two resonances may be similarly described as Fermi-polarons, sharing the fundamental principle of a neutral exciton being either bound (attractive interaction, trion-like) or unbound (repulsive interaction) to itinerant carriers [2–4, 7]. The energy separation between these peaks allows us to estimate the free carrier density as 10^{12} cm^{-2} (see Supplementary Note 1) [7]. We attribute this relatively high carrier density to electron doping from the EuS film, which we expect to be highly charged owing to the deposition technique (see Methods) [22, 23]. Measuring photoluminescence (PL) using a continuous wave laser at 1.946 eV, only a single peak is observed, attributed to the trion. The absence of neutral exciton PL is consistent with the high doping level in the flake, as is the significant Stokes shift of ~ 6 meV observed between T_{RC} and T_{PL} (Fig. 1a) [4].

When $B = \pm 8$ T, T_{RC} is only visible in one circular polarization (Fig. 1a). Owing to its spin-singlet or intervalley nature, the trion absorption strength of σ^+ (σ^-) light depends upon the itinerant carrier density in the $-K$ ($+K$) valley. Therefore, the electron Zeeman splitting is sufficiently large at this temperature to fully spin polarize the 2DEG (Fig. 1b) (see Supplementary Note 2) [3, 7]. Achieving complete spin polarization of a 2DEG of such high density as here may point to itinerant ferromagnetism, in which transient domains of oppositely spin polarized electrons at $B = 0$ T evolve into a spatially correlated spin polarized state when $B > 0$ T [24, 25]. We additionally note that while EuS is ferromagnetic, we see no evidence of magnetic proximity effects in the sample (see Supplementary Note 3).

For the next stage of the study, we incorporate the MoSe$_2$ / EuS structure into a tunable zero-dimensional microcavity (Fig. 1c), formed by introducing a downward facing top concave DBR into the optical path above the sample (as described in Ref. [26]). By control of the mirror separation using piezo nanopositioners, we tune the ground state longitudinal cavity mode (Laguerre-Gaussian LG_{00}) through resonance with both T_{PL} and T_{RC}, and perform cavity PL spectroscopy using a linearly polarized laser at power 5µW. At $B = 0$ T, we observe essentially identical PL spectra for both σ^+ and σ^- detection polarizations. As the cavity length is tuned, the observation of an anticrossing indicates strong light-matter coupling and defines upper and lower trion-polariton branches (UPB and LPB) separated by a Rabi splitting $\Omega_R \sim 9$ meV. We note here that the trion Stokes shift is comparable with the Rabi splitting, and therefore must be taken into account in order to precisely fit the polariton PL energies by going beyond the most basic coupled oscillator model (see Supplementary Note 2). Indeed, while the anticrossing originates at the energy of T_{RC}, where cavity photons are most strongly absorbed, the polariton PL shows a finite Stokes shift causing both UPB and LPB emission to tend to the trion PL energy at vanishing photon fractions. Repeating the experiment at $B = +8$ T (Fig. 1d) reveals a larger anticrossing in σ^+, while the strong coupling regime breaks down in σ^- (Ω_R is smaller than the polariton linewidths and unresolvable), consistent with the weak oscillator strength of T_{RC} in σ^- (Fig. 1a top panel), and constituting observation of valley-specific strong light-matter coupling, in which trions of opposite valley pseudospin are respectively strongly coupled to σ^+ light while only weakly coupled to σ^- light.

Fig. 2a shows polarization resolved LPB PL versus piezo voltage at $B = 0$ and $+8$ T, revealing a giant effective Zeeman splitting exceeding 10 meV, whereby the large anticrossing displayed by $+K$ valley trion-polaritons, absent for the $-K$ valley, gives rise to a clear energy separation between σ^+ and σ^- polarized modes. This occurs because the near-unity spin polarization of the 2DEG at B = +8 T suppresses the oscillator strength of the trion in σ^- polarization, by transferring it to σ^+ polarization. Fig. 2b compares the trion PL g-factor measured on the bare flake ($g = 3.9$) with that of the trion-polariton which is over 5 times larger ($g = 21.1$). While the LPB Zeeman splitting increases at higher voltages, this comes at the cost of increased polariton linewidths and reduced intensity. However, we note that the LPB Zeeman splitting exceeds the bare trion splitting for all B-field strengths and all cavity lengths studied here. This result is in marked contrast to the expected scenario in which the polariton valley Zeeman splitting is reduced relative to that of bare trion by the corresponding Hopfield coefficient [27].

Next, we show how the giant Zeeman splitting can be very effectively optically controlled. We fix $B = +8$ T and study the influence of incident laser power on the cavity PL. As can be seen in Fig. 3a, increased power re-opens the anticrossing in σ^- which previously collapsed upon application of the B-field (Fig. 1d). Fig. 3b shows trion-polariton PL spectra versus pumping power at fixed cavity length, where Ω_R grows in σ^- and correspondingly decays in σ^+, suggesting that non-resonant pumping efficiently transfers electrons between spin states (equivalently, between valley states, see Fig. 1b). Here, qualitatively, electron-hole pairs are injected by the laser and bind to form excitons and trions on ultrafast timescales (sub-ps). The initial trion population will be highly valley polarized as the only free carriers available are from the spin polarized 2DEG, however, exciton and trion valley depolarization in $MoSe_2$ is extremely efficient (ps) owing to the Maialle-Silva-Sham (MSS) mechanism (confirmed here by transient ellipticity measurements, see Supplementary Note 4) [26, 28]. Therefore, rapid intervalley scattering of trions followed by their radiative decay can result in a free electron remaining in the spin state anti-aligned to the external B-field. This means that each trion emission process results in partial transfer of electrons between spin-valley states. While trion valley relaxation occurs on ps timescales, the spin relaxation time for free electrons is $\sim$ 1000 times longer, of the order ns, as they are immune to the MSS mechanism and must undergo a large momentum transfer to scatter between spin-valley states. As such, trion intervalley scattering and subsequent photon emission can depolarize the 2DEG $\sim$ 1000 times faster than it can return to spin-polarized equilibrium. By embedding all of these processes into rate equations, we infer that laser power in the μW range is enough to fully balance the 2DEG spin populations and associated trion-polariton Rabi splittings in opposite circular polarizations. Our simulations are shown in Fig. 3c (top panel) and are in excellent agreement with experimental data.

Lastly, we relate the computed exciton and trion densities to the energy shifts of the LPB when $B = +8$ T, and deduce effective LPB interaction strengths, in this case attractive for σ^- and repulsive for σ^+. The middle panel of Fig. 3c shows the LPB blueshift in σ^+ alongside the effective interaction strength, defined as $\alpha = \partial E^+_{LPB}/\partial n^+$ (see Supplementary Note 2), which corresponds to a repulsive interaction between same-spin particles since only σ^+ excitons can depolarize electrons when $B = +8$ T. The extracted value, $\alpha \approx 0.2 \pm 0.05$ meV·μm^2 at $P = 5$ μW, is one order of magnitude larger than previously reported for trion-polaritons because it is based on a completely different mechanism [21]. It is based neither on oscillator strength or the Coulomb interaction between carriers, but instead on linear spin relaxation processes. The increase in the interaction strength at the lowest laser powers is accompanied by a marked increase in the effective trion-polariton Zeeman splitting, confirming their shared origin in the 2DEG spin dynamics (Fig. 3c bottom panel).

Our experiments demonstrate the simultaneous manifestation of strong and weak coupling regimes between a photonic mode and a many-body correlated matter excitation consisting of an exciton dressed by electrons in an effective ferromagnetic phase, resulting in a giant Zeeman splitting between trion-polariton modes. We additionally show that laser illumination acts to depolarize the 2DEG via a process of trion valley pseudospin relaxation and subsequent radiative recombination. The resulting Rabi splitting transfer between the two polarization components induces energy renormalization to which we associate large effective interactions. While in this work an EuS film was used to introduce additional free electrons into the flake, similar results should be observed in any $MoSe_2$ monolayer in which the itinerant carrier density can be raised arbitrarily to give the trion sufficient oscillator strength. Magnetic 2-dimensional materials may also be used to induce 2DEG spin polarization without the need for strong external B-fields [25]. Moreover, we note that extremely high laser powers, often pulsed and quasi-resonant, are typically needed to enter regimes of polariton non-linearity, while here the strongest effective interactions occur under low power non-resonant continuous-wave laser excitation. Our work therefore highlights doped $MoSe_2$ as a flexible system in which to realize and apply ultrastrong low-threshold nonlinearities, for instance towards TMD-based all-optical logic gates [29], or to explore nonlinear topological photonics [30].

ACKNOWLEDGEMENTS

TPL acknowledges financial support from the EPSRC Doctoral Prize Fellowship scheme under Grant Reference EP/R513313/1, and the JSPS Postdoctoral Fellowships for Research in Japan scheme. TPL, DJG, JP, YO and AIT acknowledge support from the Royal Society International Exchange Grant IEC\R3\170088. TPL, DJG, AG, CLo, LK, IA, MB and AIT acknowledge EPSRC Centre-to-Centre grant EP/S030751/1. TPL, DJG and AIT additionally acknowledge financial support of the European Graphene Flagship Project under grant agreement 881603 and EPSRC grants EP/V006975/1, EP/P026850/1 and EP/V026496/1. CLe, DS and GM acknowledge the support of the projects EU "TOPO-

LIGHT" (964770), "QUANTOPOL" (846353), of the ANR Labex GaNEXT (ANR-11-LABX-0014), and of the ANR program "Investissements d'Avenir" through the IDEX-ISITE initiative 16-IDEX-0001 (CAP 20-25). LK, IA and MB acknowledge financial support by the Deutsche Forschungsgemeinschaft through the International Collaborative Research Centre 160 (Project No. C2) and UAR professorship: Mercur Foundation (grant Pe-2019-0022). The authors thank D. N. Krizhanovskii for useful discussions.

AUTHOR CONTRIBUTIONS

TPL, DJG and JP performed low temperature magneto-optical spectroscopy. TPL, DJG, CLe, DDS, GM and AIT analyzed and discussed the bare flake and cavity spectroscopy data. CLe, DDS and GM developed the cavity fitting model and rate equations. LK and IAA collected and analyzed time-resolved data. JP and PM deposited the EuS films onto DBR substrates. TPL, DJG, JP and PM performed SQUID magnetometry. CLo identified and transferred $MoSe_2$ flakes onto EuS films. AG carried out electron density calculations. MB, YO, GM and AIT managed various aspects of the project. AIT supervised the project. TPL wrote the manuscript with contributions from all co-authors.

COMPETING INTERESTS

The authors declare no competing interests.

FIGURE CAPTIONS

REFERENCES

---

* thomas.lyons@riken.jp

† a.tartakovskii@sheffield.ac.uk

[1] Smolka, S. *et al.* Cavity quantum electrodynamics with many-body states of a two-dimensional electron gas. *Science* **346**, 332–335 (2014).

[2] Efimkin, D. K. & MacDonald, A. H. Many-body theory of trion absorption features in two-dimensional semiconductors. *Physical Review B* **95**, 035417 (2017).

[3] Back, P. *et al.* Giant paramagnetism-induced valley polarization of electrons in charge-tunable monolayer $MoSe_2$. *Physical Review Letters* **118**, 237404 (2017).

[4] Sidler, M. *et al.* Fermi polaron-polaritons in charge-tunable atomically thin semiconductors. *Nature Physics* **13**, 255–261 (2017).

[5] Tan, L. B. *et al.* Interacting polaron-polaritons. *Physical Review X* **10**, 021011 (2020).

[6] Klein, J. *et al.* Controlling exciton many-body states by the electric-field effect in monolayer MoS_2. *Physical Review Research* **3**, L022009 (2021).

[7] Roch, J. G. *et al.* Spin-polarized electrons in monolayer MoS_2 *Nature Nanotechnology* **14**, 432–436 (2019).

[8] Glazov, M. M. Optical properties of charged excitons in two-dimensional semiconductors. *Journal of Chemical Physics* **153**, 034703 (2020).

[9] Imamoglu, A., Cotlet, O. & Schmidt, R. Exciton-polarons in two-dimensional semiconductors and the Tavis-Cummings model. *Comptes Rendus. Physique* **22**, S4, 89-96 (2021).

[10] MacNeill, D. *et al.* Breaking of valley degeneracy by magnetic field in monolayer $MoSe_2$. *Physical Review Letters* **114**, 037401 (2015).

[11] Langer, F. *et al.* Lightwave valleytronics in a monolayer of tungsten diselenide. *Nature* **557**, 76–80 (2018).

[12] Ozawa, T. *et al.* Topological photonics. *Reviews of Modern Physics* **91**, 015006 (2019).

[13] Li, M. *et al.* Experimental observation of topological Z_2 exciton-polaritons in transition metal dichalcogenide monolayers. *Nature Communications* **12**, 4425 (2021).

[14] Liu, W. *et al.* Generation of helical topological exciton-polaritons. *Science* **370**, 600–604 (2020).

[15] Wang, Z., Chong, Y., Joannopoulos, J. D. & Soljačić, M. Observation of unidirectional backscattering-immune topological electromagnetic states. *Nature* **461**, 772–775 (2009).

[16] Lu, L., Joannopoulos, J. D. & Soljačić, M. Topological photonics. *Nature Photonics* **8**, 821–829 (2014).

[17] Bahari, B. *et al.* Nonreciprocal lasing in topological cavities of arbitrary geometries. *Science* **358**, 636–640 (2017).

[18] Nalitov, A. V., Solnyshkov, D. D. & Malpuech, G. Polariton Z topological insulator. *Physical Review Letters* **114**, 116401 (2015).

[19] Klembt, S. *et al.* Exciton-polariton topological insulator. *Nature* **562**, 552–556 (2018).

[20] Song, W. *et al.* Breakup and recovery of topological zero modes in finite non-Hermitian optical lattices. *Physical Review Letters* **123**, 165701 (2019).

[21] Emmanuele, R. P. A. *et al.* Highly nonlinear trion-polaritons in a monolayer semiconductor. *Nature Communications* **11**, 3589 (2020).

[22] Keller, J. *et al.* Controlling the magneto-transport properties of EuS thin films. *IEEE Transactions on Magnetics* **38**, 2673–2675 (2002).

[23] Grzeszczyk, M. *et al.* The effect of metallic substrates on the optical properties of monolayer $MoSe_2$. *Scientific Reports* **10**, 4981 (2020).

[24] Roch, J. G. *et al.* First-order magnetic phase transition of mobile electrons in monolayer MoS_2. *Physical Review Letters* **124**, 187602 (2020).

[25] Lyons, T. P. *et al.* Interplay between spin proximity effect and charge-dependent exciton dynamics in $MoSe_2$ / $CrBr_3$ van der Waals heterostructures. *Nature Communications* **11**, 6021 (2020).

[26] Dufferwiel, S. *et al.* Valley-addressable polaritons in atomically thin semiconductors. *Nature Photonics* **11**, 497–501 (2017).

[27] Lundt, N. *et al.* Magnetic-field-induced splitting and polarization of monolayer-based valley exciton polaritons. *Physical Review B* **100**, 121303(R) (2019).

[28] Glazov, M. M. *et al.* Exciton fine structure and spin decoherence in monolayers of transition metal dichalco-

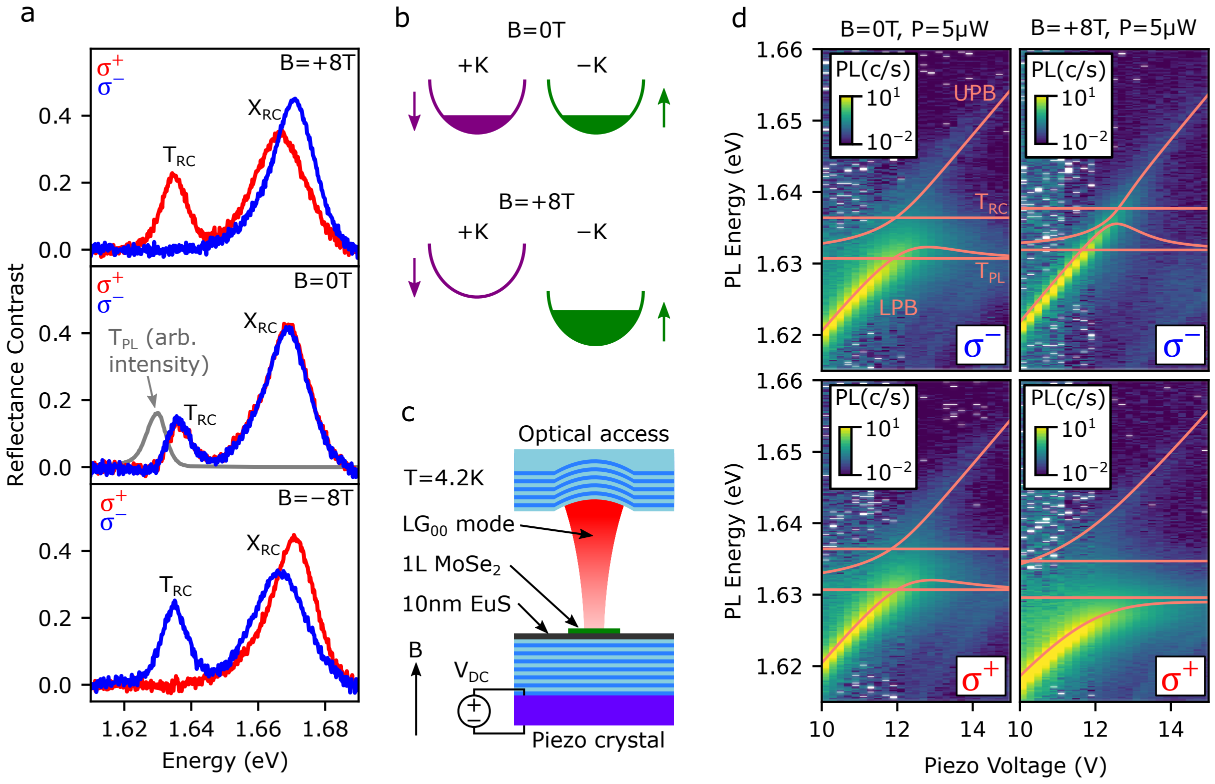

FIG. 1. **Excitations of a 2-dimensional electron gas strongly coupled to light in monolayer MoSe$_2$.** (a) Reflectance contrast RC $= (R_0 - R)/R_0$ from monolayer MoSe$_2$ (reflectance R on flake and R_0 on substrate) with raised itinerant carrier density at T $= 4.2$ K and B $= -8, 0, +8$ T. Two peaks are attributed to the neutral exciton (X_{RC}) and charged exciton or trion (T_{RC}). At high B-fields the trion absorption is completely suppressed in one or the other circular polarization of light. For comparison the trion photoluminescence T_{PL} signal at $B = 0$ T is also shown, revealing a Stokes shift of ~ 6 meV. Neutral exciton emission is absent owing to the raised doping level of the flake and rapid trion formation. (b) Sketch of the lowest conduction sub-bands of monolayer MoSe$_2$, in which the electronic spin and valley pseudospin ($+K$ or $-K$ valley of momentum space) are strictly correlated. These degrees of freedom are distinct in that the spin couples to magnetic field, while the valley pseudospin couples to light. Optical selection rules dictate that excitons and trions of $+K$ ($-K$) valley pseudospin couple, weakly or strongly, to σ^+ (σ^-) polarized photons. At $B = 0$ T, the 2DEG has zero net spin polarization. At $B = +8$ T, the 2DEG is completely spin polarized, causing the oscillator strength of the $-K$ valley trion to be suppressed owing to a lack of itinerant electrons in the $+K$ valley. (c) Schematic of the zero-dimensional open cavity structure used in this work. Applying a DC voltage to the piezo crystal decreases the cavity length (see Methods). (d) Cavity PL intensity maps (counts/s, logarithmic scale) as the cavity mode is tuned through the trion resonances. Shown are the results at $B = 0$ T (left panels) and $B = +8$ T (right panels) in both photon emission helicities. The laser is linearly polarized. At $B = 0$ T, the spectra are essentially identical between both polarizations, while the near-unity spin polarization of the 2DEG at $B = +8$ T causes strong coupling to break down in σ^- polarization. A modified coupled oscillator model incorporating the trion-polariton Stokes shift was used to fit the UPB and LPB (overlaid orange curves). The energies of T_{PL} and T_{RC} in both polarizations (orange horizontal lines) are obtained directly or inferred from bare flake spectra at $B = 0$ T and +8 T. The UPB becomes progressively dimmer at higher energies owing to increasing absorption from the EuS film.

genides. *Physical Review B* **89**, 201302(R) (2014).
[29] Amo, A. *et al.* Exciton-polariton spin switches. *Nature Photonics* **4**, 361–366 (2010).
[30] Smirnova, D., Leykam, D., Chong, Y. & Kivshar, Y. Nonlinear topological photonics. *Applied Physics Reviews* **7**, 021306 (2020).

METHODS

Low temperature magneto-optical spectroscopy

Magneto-optical spectroscopy at 4.2 K was performed by mounting the sample in a liquid helium bath cryostat with a superconducting magnet and free space optical access. Reflectance contrast measurements were performed by directing broadband white light in either σ^+ or σ^- circular polarization onto the sample and measuring the re-

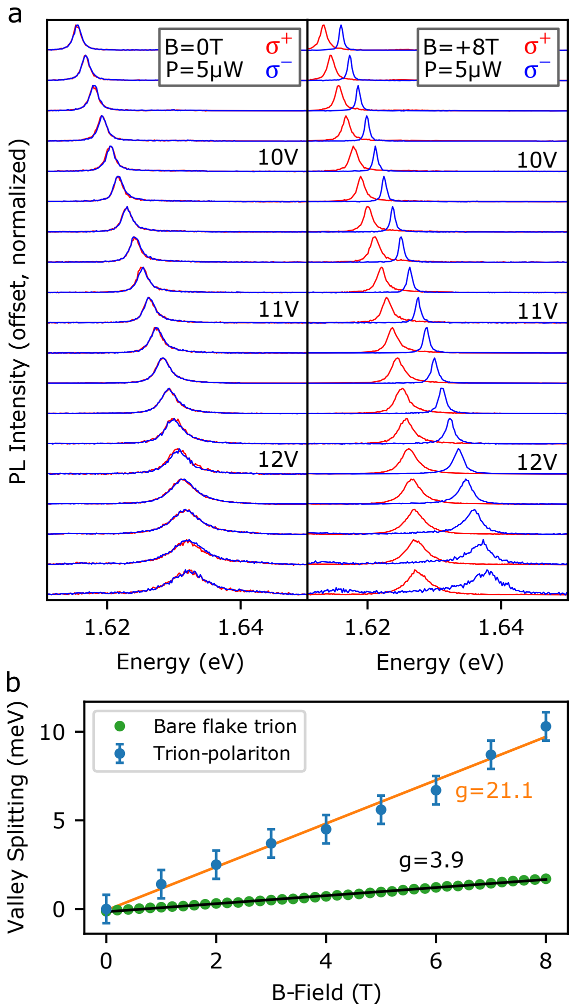

FIG. 2. **Giant effective trion-polariton Zeeman splitting.** (a) Cavity PL spectra at increasing piezo voltages (decreasing cavity length) for $B = 0$ T (left panel) and $B = +8$ T (right panel). A giant Zeeman splitting of the lower polariton branch (LPB) can be seen when the B-field is applied. Spectra normalization factors at $B = +8$ T are stable around ~ 1.2 from 9.2 V to 11.6 V, increasing to 6.6 at 12.8 V owing to onset of absorption from the EuS film, which reduces the cavity Q-factor and weakens σ^- intensity. (b) The maximum valley splitting of the trion-polariton LPB as a function of applied B-field strength. Here, we extract an effective maximum LPB Zeeman splitting at each 1 T B-field increment from our cavity fitting procedure (see Supplementary Note 2). Error bars quantify the uncertainty arising from fitting the spectral PL peaks to Lorentzian functions to extract peak energies. For comparison the valley Zeeman splitting of the bare (uncoupled) trion is also shown. The g-factors of the trion-polariton and bare trion are (21.1 ± 0.9) and (3.93 ± 0.04), respectively.

flected signal on the MoSe$_2$ monolayer (R) and adjacent bare EuS film (R_0), and calculating the RC $= \Delta R/R$. Photoluminescence spectroscopy was performed by directing a linearly polarized continuous wave laser at 1.946 eV onto the sample and detecting the emission in either σ^+ or σ^- circular polarization. For both RC and PL the signal was directed through a single mode fiber to a 0.75 m spectrometer and onto a nitrogen-cooled high sensitivity charge-coupled device (see Supplementary Note 5).

The tunable zero-dimensional open microcavity is formed by bringing a concave top DBR into the optical path above the planar bottom DBR, on top of which is the 10 nm EuS film and monolayer MoSe$_2$. The EuS film serves to increase the itinerant electron density in the MoSe$_2$. A gap filled with helium exchange gas separates the DBRs forming a zero-dimensional optical microcavity. Piezo nanopositioners allow precise tuning of the cavity length, whereby applying a DC voltage will decrease the cavity length and increase the energy of the ground state zero-dimensional Laguerre-Gaussian mode (LG$_{00}$) such that it can be tuned through resonance with both T_{PL} and T_{RC}.

Europium sulfide deposition

A 10 nm thick film of europium sulfide (EuS) was deposited onto a dielectric DBR (top layer SiO$_2$) by electron-beam evaporation. By maintaining a low substrate temperature of 16 °C during the deposition, we ensure that the resulting EuS film will be sulfur deficient, owing to the much lower vapor pressure of S relative to Eu, causing S atoms to re-evaporate from the substrate during growth. The resulting sulfur vacancies act as electron donors causing the non-stoichiometric EuS film to act as a heavily-doped ferromagnetic semiconductor [22]. The MoSe$_2$ monolayer therefore becomes highly charged when it is stamped on top of the EuS substrate [23].

Sample fabrication

A MoSe$_2$ bulk crystal supplied by HQ Graphene was exfoliated with tape onto a polydimethylsiloxane (PDMS) sheet, and a suitable monolayer identified by optical microscopy. This monolayer was then stamped onto the DBR / EuS substrate using a conventional viscoelastic dry transfer method.

Data Availability

Data supporting the plots within this paper is available from the corresponding authors upon request.

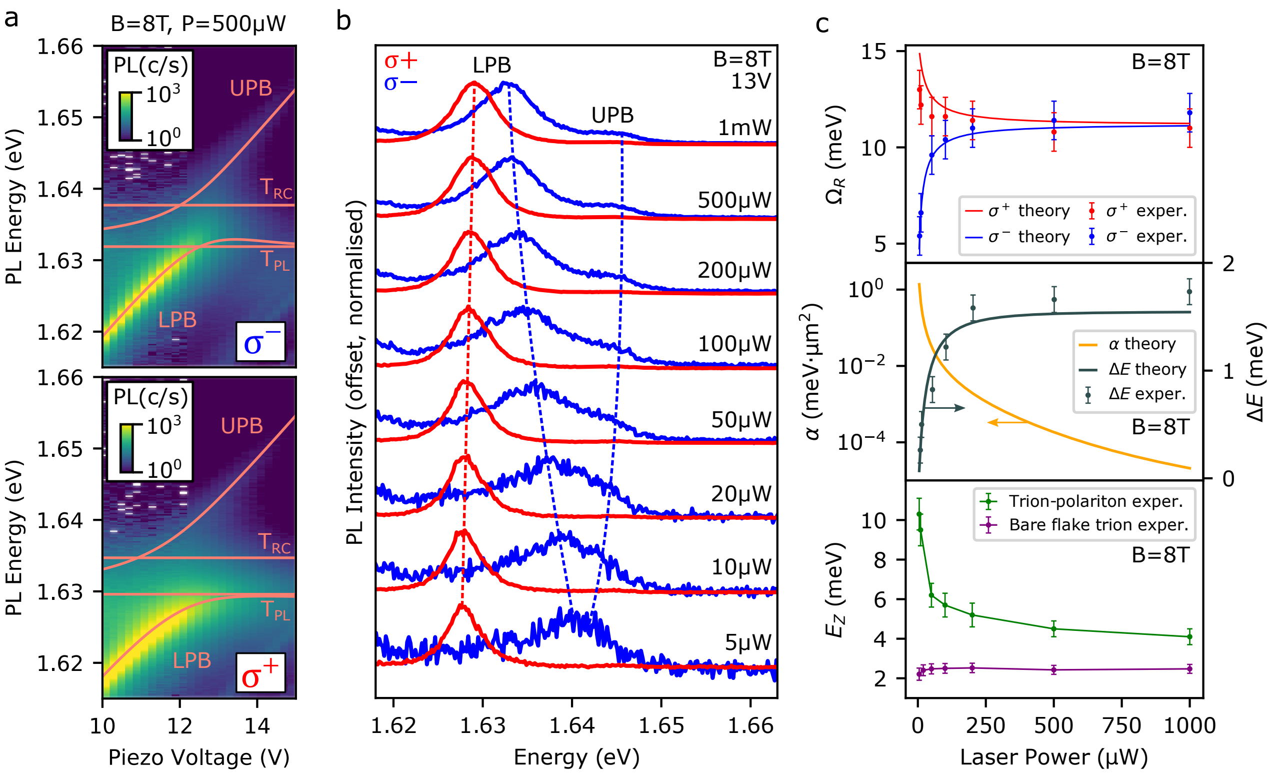

FIG. 3. **Trion-polariton effective nonlinearity.** (a) Cavity PL intensity colormaps (counts/s, logarithmic scale) in σ^+ and σ^- emission at $B = +8$ T and a high laser power $P = 500$ µW. An anticrossing is seen in both polarizations despite the strong applied B-field. Polariton fitting curves incorporating the Stokes shift are overlaid. (b) Cavity PL spectra at fixed detuning close to trion-cavity resonance, at B = +8 T, taken at varying incident laser powers. As the power is decreased, the 2DEG spin polarization increases and the anticrossing in σ^- is suppressed. This has the secondary effect of amplifying the effective Zeeman splitting between σ^+ and σ^- lower polaritons. (c) (top panel) Rabi splittings, Ω_R, in σ^+ and σ^- at B = +8 T against laser power. Nonlinear breakdown of strong coupling in σ^- is observed as the power is decreased. Solid curves are simulated results (see Supplementary Note 2). (middle panel) The calculated effective trion-polariton interaction strength, α (see main text for definition), and the calculated and experimental blueshift, ΔE, of the LPB in σ^+ polarization, both at B = +8 T as a function of pump power. As there is no emission at 0 µW, the blueshift between 0 and 5 µW is assumed to be the same as between 5 and 10 µW, measured as (0.23 ± 0.12) meV. (lower panel) The maximum LPB Zeeman splitting, E_Z, at B = +8 T against laser power. The splitting increases drastically at the lowest powers when the 2DEG spin polarization is highest. For comparison the bare trion Zeeman splitting is shown. Error bars on experimental data points quantify the uncertainty arising from fitting spectral PL peaks to Lorentzian functions to extract peak energies.